Pedestrian Virtual Space Based Abnormal Behavior Detection

Yepeng Guan ,Wenqing Mao

Abstract: It is a crucial issue to efficiently detect anomaly from surveillance videos. Abnormal behavior detection is developed in an unsupervised way based on spatio-temporal motion analysis in pedestrian virtual space. The pedestrian virtual plane is constructed which consists of both the ground plane and the pedestrian head one. The abnormal behavior is discriminated by a circular variance of pedestrian trajectories around the 3D virtual region instead of traditional 2D protected one. The protected region can be assigned as different shapes and sizes. Experiments show that the proposed method is efficient for distinguishing the anomaly in a protected region without any hypothesis for the scenario contents in advance. Comparisons with state-of-the-arts highlight the superior performance of the proposed method.

Keywords: abnormal behavior detection; spatio-temporal motion analysis; pedestrian virtual space; circular variance

I Introduction

Abnormal movement around some important protected regions, as a kind of serious safety issues, is getting more and more attention. The protected region is often considered as a highly concerned one in the reality scene including some entrances of military authorities, important institutes and so on.

Video surveillance has become one of the popular ways in detecting pedestrian movement behavior and providing security alert timely. Based on the video frames captured by the camera, some abnormal activities, uncommon behaviors, or irregular events in a scene can be distinguished [1-2]. One of the key problems is how to detect pedestrians efficiently from videos. Many methods [3-11] have been proposed to deal with it including utilizing shapes of objects [3-4], classifiers [5-7], moving object segmentation [8-9] and filter tracking [10-11]. These methods have two limits when dealing with detection and tracking for abnormal pedestrians. One is that they are not suitable for abnormal pedestrian detection since the pedestrian's morphology changes frequently. The other is that it's difficult to detect and track multiple pedestrians because of their occlusion and complex motion patterns. Another key issue is how to distinguish abnormal motion behaviors from normal ones in videos. Many approaches have been developed to detect the anomaly including normal trajectory dictionary constructing [12] and trajectory learning framework [13]. These methods need prior training before judging abnormal behavior. It does not meet demands of real-time monitoring. Besides, it is difficult to get complete trajectories for distinguishing abnormal behavior. Because there are different trajectories for pedestrian motion around the sensitive protected region such as loitering ones. To solve this problem, some methods without training have been proposed to detect the anomaly [14-18]. Anomaly has been detected according to the position relationship of foreground pixels with specific warning line in [14-15]. These methods [14-15] are prone to be affected by pedestrian poses and scenario illumination variations. Besides, it is difficult to judge whether pedestrian passed through the specific 2D warning line or not efficiently. An intruding abnormal detection has been proposed based on the position relationship between the pedestrian center gravity and protected area instead of warning line in [16-18]. These methods [16-18] are performed in 2D image space. It is difficult to determine whether pedestrian intruded the specific region or not. To overcome some limits mentioned above, both distinct spiral and close trajectories on 2D image in [19] are employed to discriminate the anomaly. Angle change on 2D image based abnormal motion detection approach has been proposed in [20]. The limit is that only a small number of trajectories can be identified and the angle variation on 2D image has large errors. Motion history image (MHI) for the centroid of the moving pedestrian has been used in [21]. The similarity between two MHIs of template trajectories is adopted to judge the anomaly. There are some simple loops for the template trajectories [22], which cannot be used to deal with some complex trajectories in the videos. Besides, it is hard to get complete human body contours since they are occluded when multiple pedestrians move in the scene.

Aiming at some limits mentioned above, a novel abnormal motion detection method is developed based on pedestrian spatio-temporal motion around a 3D virtual space instead of traditional 2D protected region. An overall flowchart of the proposed approach is shown in Fig. 1. The 3D virtual plane equation is constructed according to single pedestrian extracted by ones head in a surveillance scenario. A corresponding 3D virtual warning space for the protected region in the scene is built. The problem whether a pedestrian intruded or loitered around the warning region in a 2D scene is transformed to the one whether he intruded or loitered around the 3D virtual warning space. The abnormal behavior is discriminated in a circular variance of pedestrian

Y.-P. Guan was born in Xiaogan, Hubei Province, China, in 1967. He did his first postdoctoral research at Southeast University in electronic science and technology. Then he did his second postdoctoral research at Zhejiang University in communication engineering, and he had been an Assistant Professor with the Department of Information and Electronics Engineering, Zhejiang University. Since 2007, he has been a Professor with School of Communication and Information Engineering, Shanghai University. He is the author of more than 120 articles, and more than 20 patents. His research interests include intelligent information perception, digital image processing, computer vision, and security surveillance and guard. E-mail: ypguan @shu.edu.cn

W.-Q. Mao was born in Chuzhou,Anhui Province,China, in 1994. She received the B.S. degrees in electrical automation from Qingdao University of Science and Technology, Qingdao, China, in 2017. She is currently pursuing a master's degree at Shanghai University. Her research direction is computer vision. E-mail: maowenqing@shu.edu.cn

moving around the virtual region instead of around 2D image plane. The proposed circular variance not only can be used to represent the remote change of the pedestrian motions, but also needs not consider the shape of pedestrian motions. Comparisons with some state-of-the-arts have highlighted the superior performance of the proposed method. The main contributions are as follows. The first contribution is that a 3D pedestrian virtual space is constructed based on detection and tracking for only one pedestrian. The pedestrian motion is mapped into a 3D virtual space instead of traditional 2D image space. The second contribution is that the circular variance of pedestrian motion is developed to distinguish the anomaly, which describes pedestrian motions no matter how long he has moved. The third contribution is that it is practical for real applications and does not require sample training or any hypothesis for the scenario contents.

The rest of the paper is organized as follows. Pedestrian 3D virtual space construction is described in Section II. Pedestrian abnormal motion analysis method is developed in Section III. Experiments and analysis are discussed in Section IV and followed by some conclusions in Section V.

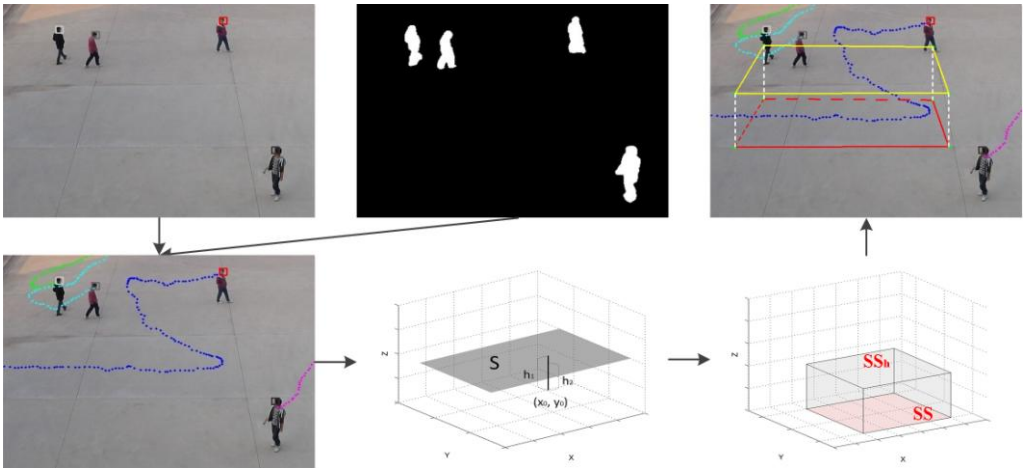

Fig.1 An overall flowchart of the proposed approach for detecting abnormal behaviors

IIPEDESTRAIN 3D VIRTIUAL SPACE CONSTRUCTION

According to our previous work in multiple heads detection and tracking [23-24], we get head vertex's coordinates (x_{h1}, y_{h1}) and shoulders' central coordinates (x_{h2}, y_{h2}). To construct a 3D pedestrian virtual plane equation, we determine only one pedestrian corresponding foot's central coordinates (x_0, y_0) and any other two points' coordinates (x_1, y_1), (x_2, y_2) on the ground at the initial stage of video surveillance. h_1 and h_2 are the distances (x_{h1}, y_{h1}) and (x_{h2}, y_{h2}) from (x_0, y_0), respectively (seen from Fig. 2).

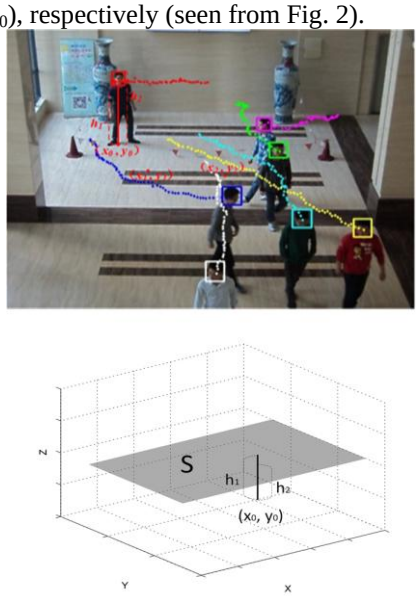

Fig.2 Pedestrian 3D virtual space model construction

Assume a ground plane equation is:

$$AX + BY + D = 0 \tag{1}$$

Based on (x_0, y_0) and other two points (x_1, y_1), (x_2, y_2) on the ground, the coefficients A, B, and D in (1) can be solved in singular value decomposition as following:

$$\begin{bmatrix} x_1 & y_1 & 1 \\ x_2 & y_2 & 1 \\ x_0 & y_0 & 1 \end{bmatrix} \begin{bmatrix} A \\ B \\ D \end{bmatrix} = 0 \tag{2}$$

Let head vertex plane equation and shoulder one are as follows, respectively:

$$AX + BY + CZ + D' = 0 \tag{3}$$

$$AX + BY + CZ + D'' = 0 \tag{4}$$

We get simultaneous equations based on A, B, D, the distances h_1, and h_2 as following:

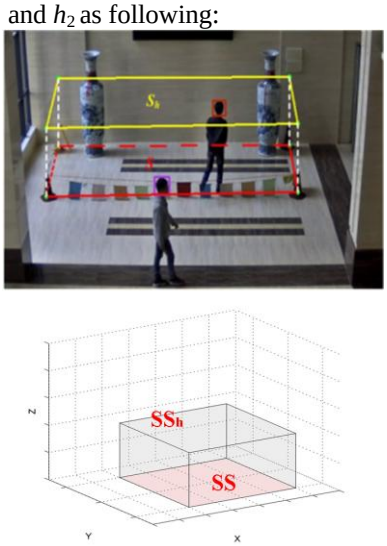

Fig.3 3D virtual space region construction based on 2D protected region

$$\begin{cases} C \times h_1 = D - D' - B \times h_1 \\ C \times h_2 = D - D'' - B \times h_2 \end{cases} \tag{5}$$

Let $r = \frac{h_2}{h_1} = \frac{D - D'' - B \times h_2}{D - D' - B \times h_1}$, the coefficients C, and D' in (3) can be solved as

$$\begin{bmatrix} h_1 & 1 \\ h_2 & r \end{bmatrix} \begin{bmatrix} C \\ D' \end{bmatrix} = - \begin{bmatrix} Ax_{h1} + By_{h1} \\ Ax_{h2} + By_{h2} + r(Bh_1 - D) + D - Bh_2 \end{bmatrix} \quad (6)$$

Based on the pedestrian plane equations mentioned above, a 2D protected region S in video surveillance image is transformed into a 3D virtual space (shown in Fig.3). The ground protected area SS in the 3D space corresponds to 2D region S, SS_h is the pedestrian shoulders plane. The space between SS and SS_h is a 3D virtual protected region.

III PEDESTRIAN ABNORMAL MOTION ANALYSIS

The term anomaly cannot be defined explicitly [25]. Some methods have been developed based on the implicit assumption that events occur occasionally are potentially abnormal, and taken as anomaly [26-28]. We focus on recognizing whether pedestrian intruded a specific region or loitered around the region.

A.Intruding Anomaly Detection

One of the key problems is how to determine whether pedestrian passed through the protected region or not. A common simple method has been employed to detect intrusion as following.

Some features of corresponding objects are extracted after segmenting foreground regions for each frame including motion foreground size (S), and center of mass (C_e) of the object. For S, we just calculate the number of pixels of foreground. C_e can be estimated as:

$$Ce = (\sum_{i=1}^{S} x_i / S, \sum_{i=1}^{S} y_i / S) \quad (7)$$

where x_i and y_i are the location of foreground on x and y axis, respectively.

It can be judged whether there is intrusion or not as:

$$I = \begin{cases} 1, if \ \ Ce \in R \\ 0, otherwise \end{cases} \quad (8)$$

where the R represents the protected region.

Some examples for some pedestrian walked in different scenarios are shown in Fig.4.

The pedestrian labeled as “1” would be judged that he intruded into the protected region (shown in red frame in Fig.4) if the method as mentioned above is adopted. In fact, no any pedestrian stepped into the protected region.

To address this problem, we transfer the 2D intruding anomaly detection to the 3D virtual region. A projection strategy is developed as follows.

Let a projection ray L start from central point P of pedestrian head and link with any endpoints of manual warning region S. We compute the sum C_o of cross points that ray L intersects the polygon S as:

$$Co = \begin{cases} Co + 1, \text{if } L \text{ I } l_i \\ Co, \text{otherwise} \end{cases} \quad (9)$$

where $l_i (i=1, \cdots, k)$ is a side of the polygon S, $L \text{ I } l_i$ indicates that L intersects with l_i.

Fig.4 Some examples for intruding in a 2D region

We determine whether the point P locates in the polygon S or not as following:

$$\delta(P,S) = \begin{cases} 1, \text{if } Co\%2 = 1 \\ 0, \quad \text{otherwise} \end{cases} \quad (10)$$

where the symbol % is a modulo operator.

If $\delta(P, S) = 1$, it means that the P is inside S, which indicates that pedestrian intruded the specific warning region.

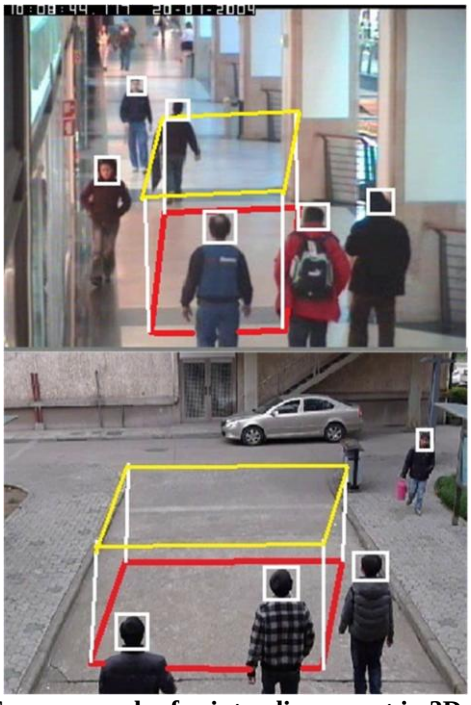

Fig.5 Some examples for intruding or not in 3D virtual region

Some examples are given in Fig.5 that 3D virtual regions are constructed according to the previous 2D protected regions (shown in Fig.4). No any pedestrians including the one labeled as “1” would not be taken as intruders that he stepped into the protected regions if (10) is employed. Some results would be further discussed later.

B.Loitering Anomaly Detection

Let the set of direction angle of pedestrian trajectory be $A_i = \{\alpha_1, \alpha_2, ..., \alpha_i\}$. Each direction α_i is computed as:

$$\alpha_i = \arctan(y_i - y_{i-1}, x_i - x_{i-1}) \quad (11)$$

A common method can used to determine whether pedestrian is loitering or not according to the angle variation. There are diverse motions trajectories for pedestrians. Some examples are given in Fig. 6.

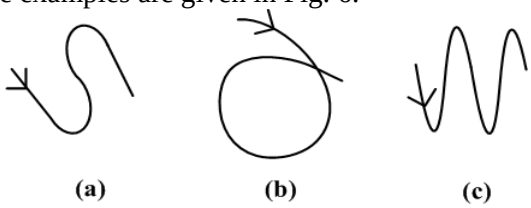

Fig.6. Some examples for pedestrian motion trajectories

It would be difficult to determine whether pedestrian is loitering or not in the angle variation. For example, α changed from 0° to 340°, the direction variation is 170°. It would not be any motion shapes for pedestrian in this way.

The circular variance (*Cv*) [29] is employed to estimate pedestrian motions.

An angle buffer is introduced to store direction angle α_i for calculating *Cv*. Let the size of angle buffer be *k*. *Cv* is calculated as following:

$$Cv = 1 - \frac{\sqrt{[\sum_{t=i-k}^{i} \sin(a_t)]^2 + [\sum_{t=i-k}^{i} \cos(a_t)]^2}}{k} \quad (12)$$

The larger *Cv* is, the higher the degree of motion direction change is. Some examples for pedestrian loitering randomly in a scenario are shown in Fig. 7.

One can find that pedestrian loitered in different trajectories from left columns in Fig.7. Correspondingly, the *Cv* curve presents different variation shapes, respectively. The value of *Cv* is low when motion direction changes gently while it is high when direction changes rapidly.

From Fig.7, we can see the peak value of *Cv* is different when direction is changing rapidly or gently. We calculate the variation of *Cv* as follows:

$$Sym(Cv_i) = (Cv_{i+k} - Cv_i)(Cv_i - Cv_{i-k}) \quad (13)$$

where Cv_i, Cv_{i+k} and Cv_{i-k} are computed as (12) according to $\{\alpha_{i-k}, \alpha_{i-k+1}, \ldots, \alpha_i\}$,$\{\alpha_i, \alpha_{i+1}, \ldots, \alpha_{i+k}\}$ and $\{\alpha_{i-2k}, \alpha_{i-2k+1}, \ldots, \alpha_{i-k}\}$, respectively.

$Sym(Cv_i)$ is used to represent the change of the slope of Cv_i. If $Sym(Cv_i) < 0$, it illustrates that the slope of Cv_i was changed. Otherwise if $Sym(Cv_i) > 0$, the slope of Cv_i has not been changed.

The variation numbers of Cv_i slope is calculated as:

$$Cc = \begin{cases} Cc+1, & \text{if } Sym(Cv_i)Sym(Cv_{i-1}) < 0 \\ 0, & \text{otherwise} \end{cases} \quad (14)$$

In order to further determine whether pedestrian is loitering around the protected region or not, we consider the distance between the pedestrian and the protected area as following.

$$dist(p, r) = \min(dist(p, L_i)) \; i = 1,2,...,n \quad (15)$$

where L_i is a side of a protected region, and *n* is the number of edges of protected one, and symbol min is a minimal operator.

The abnormal motion is defined as:

$$\lambda(Cc, T) = \begin{cases} 1, if \; Cc \geq T \\ 0, otherwise \end{cases} \quad (16)$$

where *T* is a threshold value and would be discussed later.

IV EXPERIMENTS AND ANALYSIS

To test performance of the proposed method, we experiment in some real-world video sequences. Collected video datasets by ourselves are selected to test the performance at the same situations. All the experiments are performed in C++ with OpenCV, Pentium(R) 2.6GHz CPU and 2G RAM.

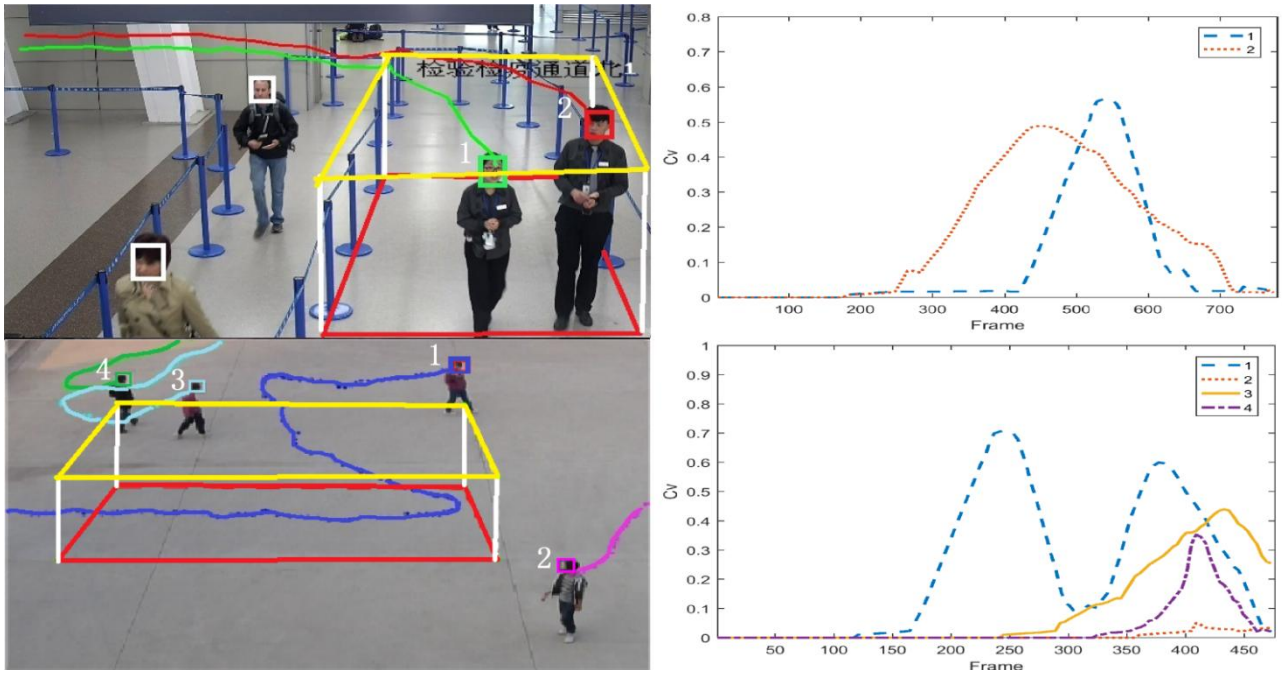

Fig.7 *Cvs* in different scenes as *k*=30. Left columns are pedestrian trajectories in the scenes, right columns are corresponding *Cvs*.

A. Tested Videos

The first video is captured in a vertical angle with resolution 640×480 pixels outdoors and labeled as Seq.1. There are multiple pedestrians in this video sequence. Some of pedestrians loitered randomly and others walked along different paths in a square in Seq.1.

The second video near the park is also captured in a vertical angle with 640×480 pixels and labeled as Seq2. There are multiple pedestrians in this video sequence. Some people loitered around the protected area at random, and some people stepped directly into the protected area.

The last video is a surveillance video in a customs checkpoint and labeled as Seq.3. Most of pedestrian walk along the prescribed channel, while some ones walked through the forbidden area.

One can download free these videos from http://pan.baidu.com/s/1gfGaCeB for non-commercial academic research. Some examples for these videos are given in Fig.8.

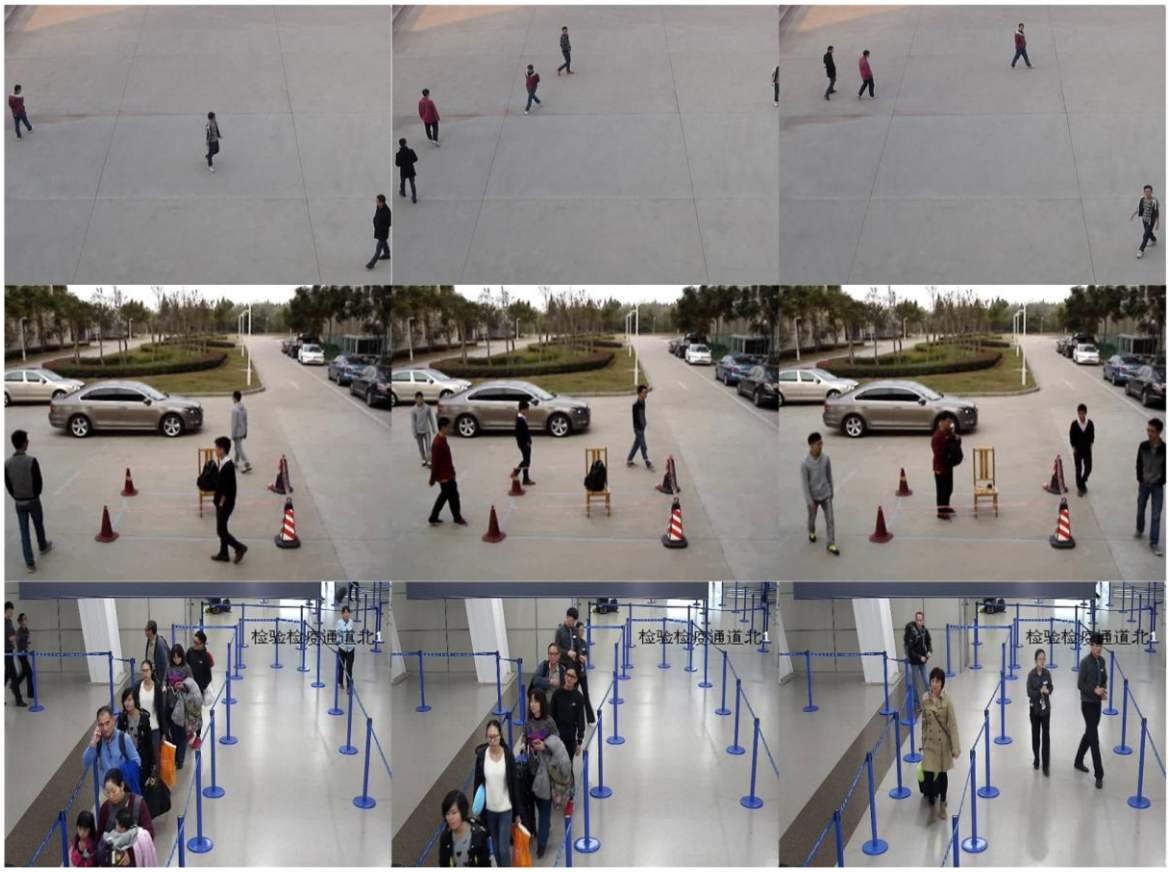

Fig.8 Some examples of the tested videos labeled as Seq.1, Seq.2, Seq.3 from top to bottom, respectively.

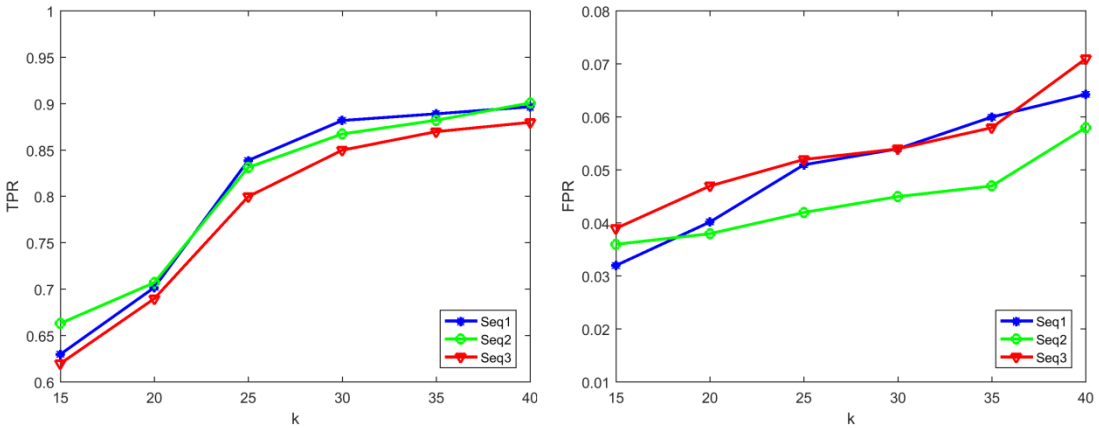

Fig.9 TPR and FPR with different *k*s

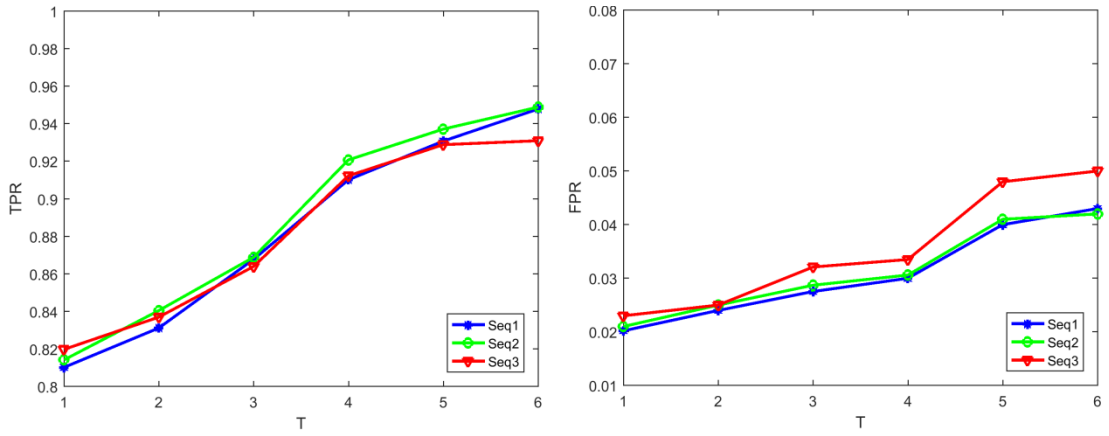

Fig.10 *TPR* and *FPR* with different *T*s

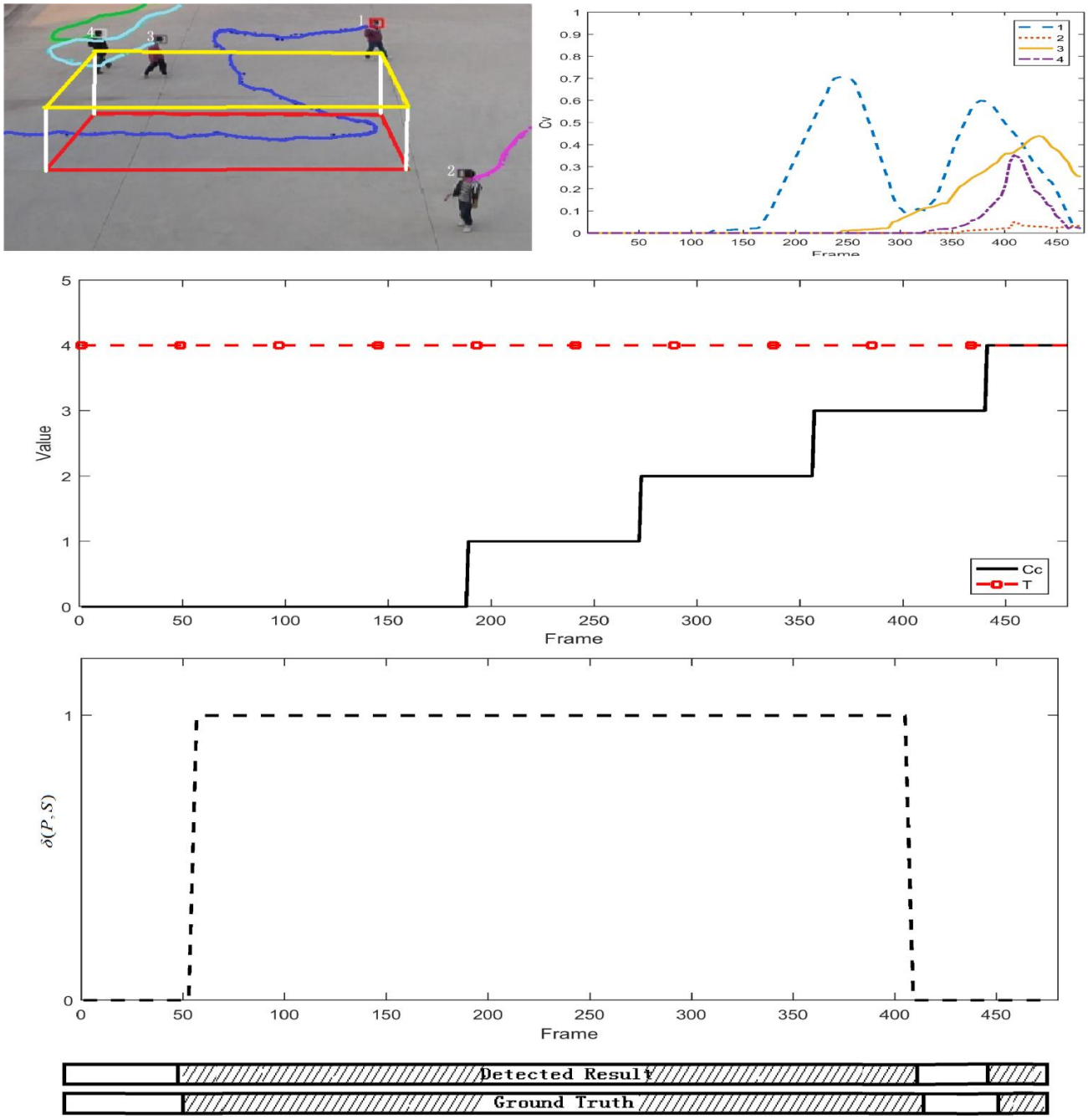

Fig.11. Some results from Seq.1. Some pedestrians loitered around a specific region in a square, others walked randomly with different trajectories, corresponding Cv, Cc, and δ(P, S) curves, both anomalies detected results and ground truth marked as blank bar, from top to bottom, right to left, respectively.

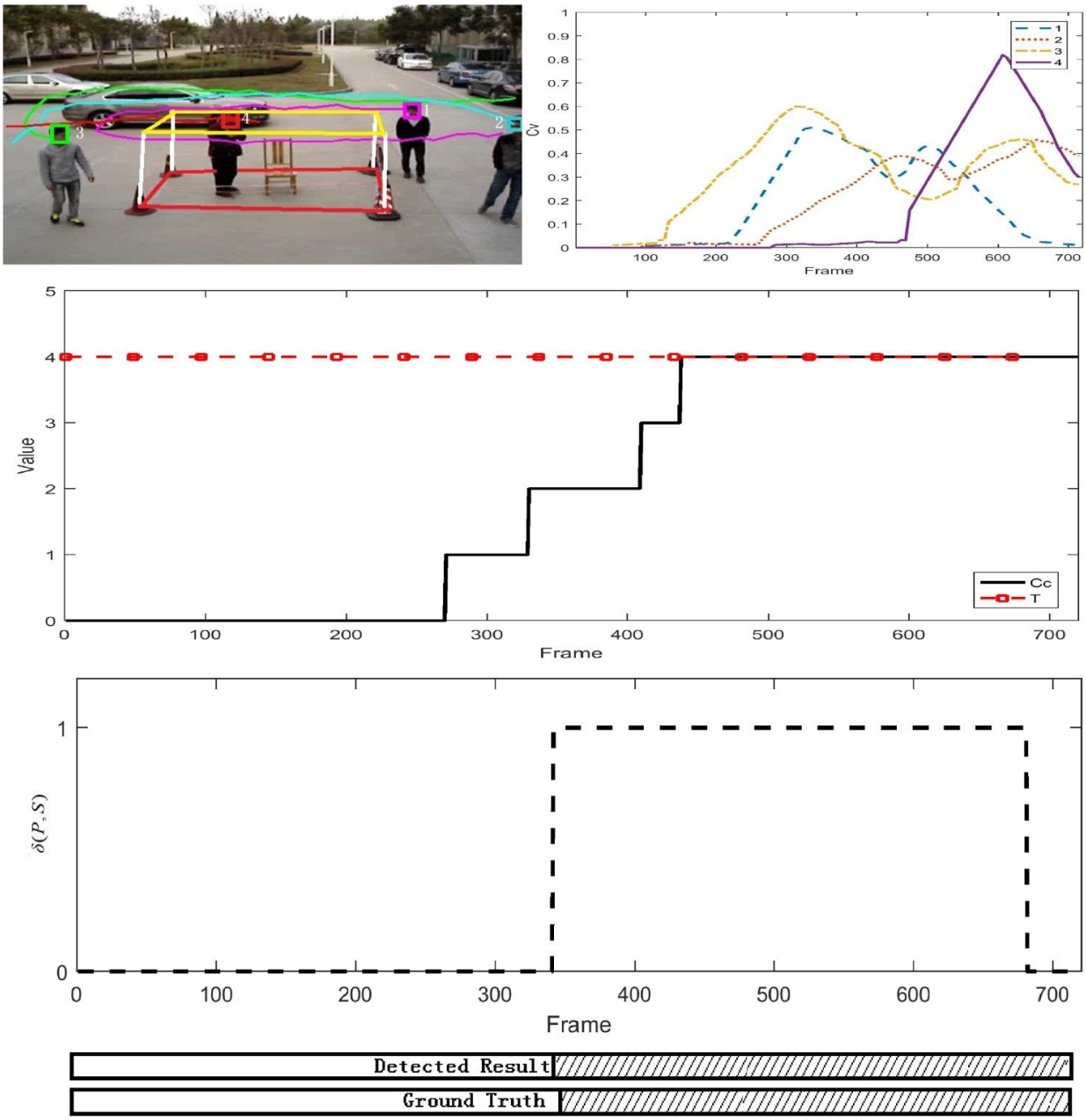

Fig.12. Some results from the Seq.2. Pedestrian loitered around a park and passed through a specific region along a cement road with motion trajectory, corresponding *Cv*, *Cc*, and *δ*(*P*, *S*) curves, both anomalies detected result and ground truth marked as blank bar, from top to bottom, right to left, respectively.

B.Choice of Parameters

To build a fair comparison, k in (12) and T in (16) are kept the same in the experiment. For k in (12), if it is small, the corresponding motion information may be insufficient to describe pedestrian motion patterns. Otherwise, some adjacent patterns will be affected each other. To get a reasonable k, we change it from 15 to 40 at an interval of 5 to evaluate its performance by receiver operating characteristic (ROC) [30-31].

All tested videos are selected to perform parameter analysis. Some results are shown in Fig.9. One can note that both true positive rate (TPR) and false positive rate (FPR) increase with the increasing of k from Fig.9. We set k to 30 as a tradeoff between TPR and FPR and keep it the same in the experiment.

For T in (16), we change it from 1 to 6 at an interval of 1 and evaluate the performance as mentioned above. Some results are shown in Fig.10 for the tested videos.

We set T to 4 as a trade-off between the TPR and FPR for all the videos and keep it the same in the experiment.

C.Performance Comparisons with Some State-of-The-Arts

Some pedestrians loitered randomly and others walked along different paths in a square in Seq.1. Some results for pedestrian motion trajectories and motion behavior judgments are shown in Fig.11. Both the intruding and loitering anomalies are detected when they walked into a specified region according to $\delta(P, S) = 1$ or loitered around the specified one according to $Cc \geq 4$. One can find that the detected results are in keeping with the ground-truth from Fig.11

.

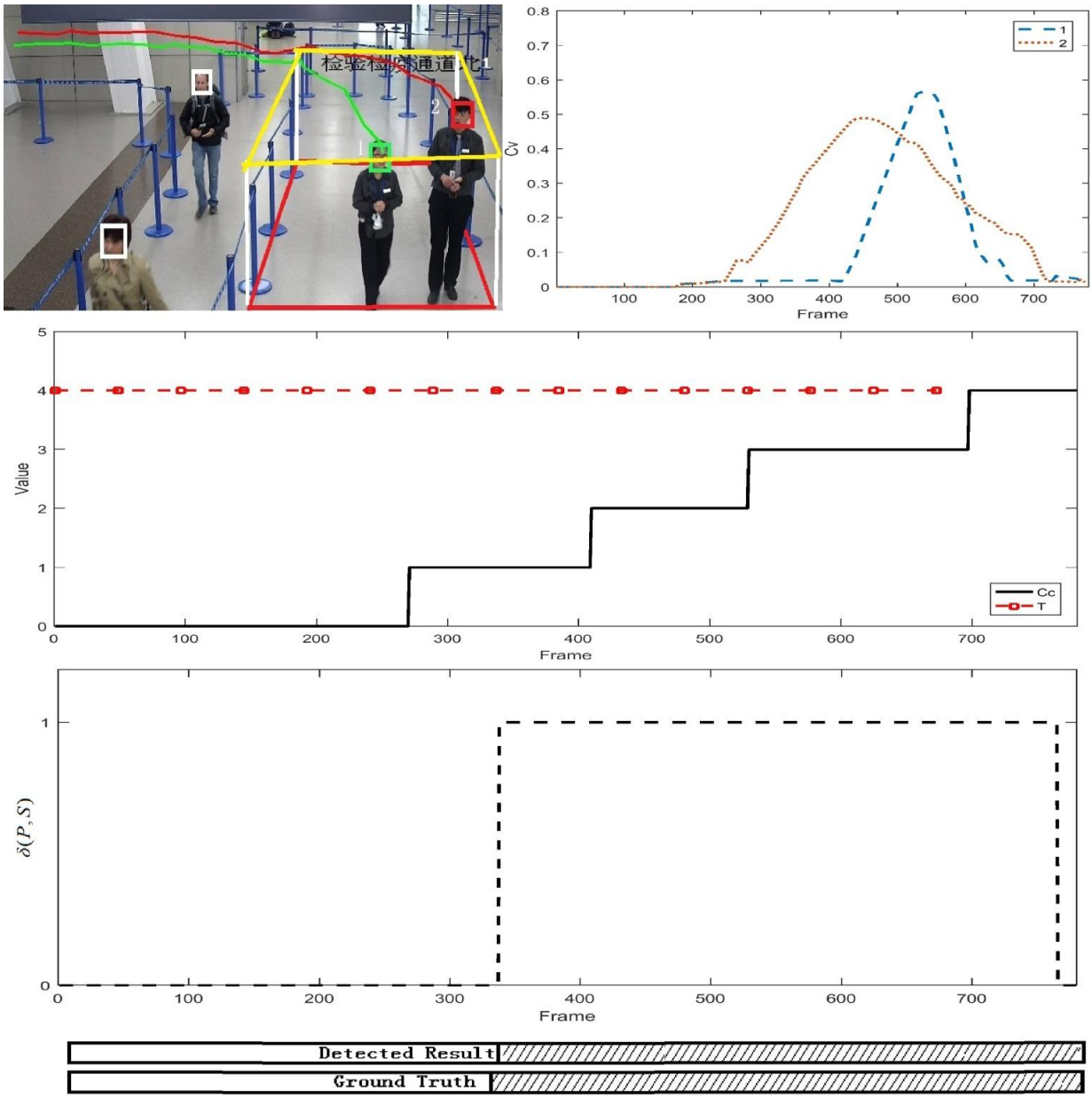

Fig.13. Some results from the Seq.3. Pedestrian loitered around a hall and passed through a specific region with motion trajectory, corresponding *Cv*, *Cc*, and *δ*(*P*, *S*) curves, both anomalies detected result and ground truth marked as blank bar, from top to bottom, right to left, respectively.

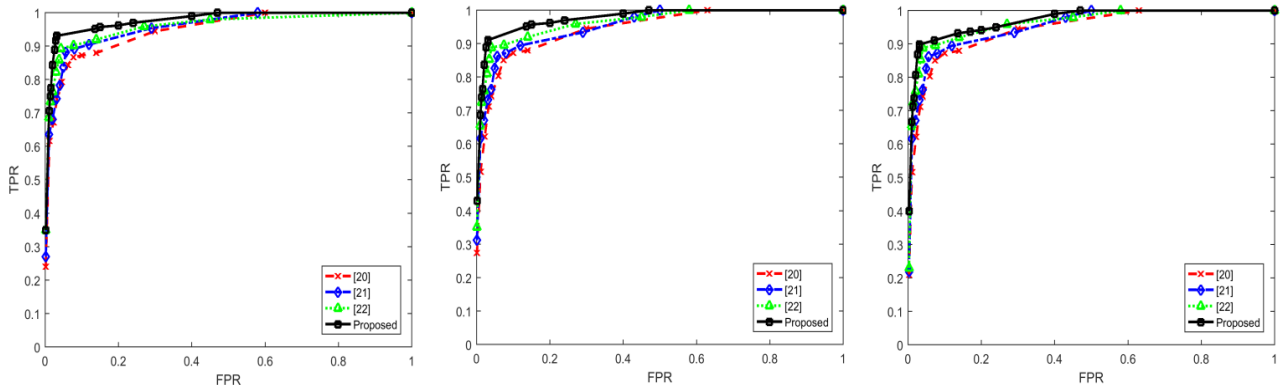

Fig.14 Comparisons among the investigated methods in all videos, and they are the results of Seq.1, Seq.2, Seq.3 from left to right, respectively

Multiple pedestrians loitered around a park and someone passed through the road-block region in Seq.2, which makes the anomaly judgment be challenging. Some results are shown in Fig.12. One can find that the detected results are in accordance with the ground-truth from Fig.12.

Most pedestrians walk along the prescribed passages, while someone cross into "no-go" region. Some results are shown in Fig.13. One can find that the detected results are corresponding to the ground-truth also from Fig.13.

In order to evaluate further the performance of the proposed method, some methods have been selected to test the performance at the same conditions including [20-22]. Some quantitative results in different methods for the above tested videos are shown in Fig.14, respectively. One can note that the propose method has superior performance by comparisons. Some performance comparisons are given in Table I.

Table I. Comparisons in anomaly detection

Methods	TPR	FPR
[20]	84.23%	7.48%
[21]	87.08%	5.89%
[22]	87.90%	4.55%
Proposed	**91.14%**	**3.13%**

In order to further evaluate the performance in processing times and build a fair comparison, all videos are kept the original size of corresponding videos. Some results of the average running time for each frame in the selected videos are given in Table II.

One can find that the proposed method has superior processing performance among the investigated approaches from Table II.

Table II. Comparisons in average process times (ms)

Methods	[20]	[21]	[22]	**Proposed**
Seq.1	120	135	130	**110**
Seq.2	150	170	160	**150**
Seq.3	190	200	195	**170**

By comparisons, it highlights that the proposed approach has superior performance among the investigated methods in distinguishing the difference between the normality and anomaly even if in the case of multiple pedestrian with different motions from the beginning to the end in the video sequence.

V CONCLUSIONS

Abnormal behavior detection is developed in an unsupervised way based on spatio-temporal motion analysis in pedestrian virtual space. The 3D pedestrian virtual space is constructed based on detection and tracking for only one pedestrian. The pedestrian motion pattern is mapped into 3D virtual space instead of traditional 2D image space. A circular variance of pedestrian motion around the 3D virtual region which described the 3D trajectory is developed to distinguish the anomaly, which describes the pedestrian motions no matter how long he has moved. The protected region can be assigned as different shapes and sizes. Anomaly detection is practical for real applications and does not require sample training or any hypothesis for the scenario contents. Experiments highlight that the proposed approach is efficient for distinguishing the anomaly without any hypothesis for the scenario contents in advance. Comparisons with some state-of-the-arts have indicated the superior performance of the proposed method.

Acknowledgments

This work is supported in part by the Natural Science Foundation of China (Grant no. 11176016, 60872117), and Specialized Research Fund for the Doctoral Program of Higher Education (Grant no. 2012108110014).

References

[1] Zhang, Y., Lu, H. and Zhang, L. *et al*. "Video anomaly detection based on locality sensitive hashing filters." Pattern Recognition, 2016, 59(S1): 302-311.

[2] Okusa, Kosuke and Toshinari, K. "Human gait modeling and statistical registration for the frontal view gait data with application to the normal/abnormal gait analysis", Lecture Notes in Electrical Engineering, 2014, 247: 525-539.

[3] Shen, J., Zuo, X. and Yang, W. *et al*. "Learning discriminative shape statistics distribution features for pedestrian detection." Neurocomputing, 2016, 184(S1): 66-77.

[4] Ma, Q. and Nie, D. "Object detection algorithm based on multiple shape templates." Journal of Information and Computational Science, 2016, 7(11): 2309-2315.

[5] Sugimura, D., Takayuki, F. and Fujimura, T. *et al*. "Enhanced Cascading classifier using multi-scale HoG for pedestrian detection from aerial images." International Journal of Pattern Recognition and Artificial Intelligence, 2016, 30(3): 1655009-1655032.

[6] Devanne, M., Berretti, S. and Pala, P. *et al*. "Motion segment decomposition of RGB-D sequences for human behavior understanding." Pattern Recognition, 2017, 61(S1): 222-233.

[7] Aguilar, W., Luna, M. and Moya, J., *et al*. "Pedestrian detection for UAVs using Cascade classifiers with meanshift", Proceedings of IEEE International Conference on Semantic Computing, 2017: 509-514.

[8] Cai, Y., Sun, X. and Wang, H., *et al*. "Night-time vehicle detection algorithm based on visual saliency and deep learning." Journal of Sensors, 2016, 2016(1):1-7.

[9] Guan, Y. "Spatio-temporal motion-based foreground segmentation and shadow suppression." IET Computer Vision, 2010, 4(1): 50-60.

[10] Qiao, M., Wang, T. and Dong, Y., *et al*. "Real time object tracking based on local texture feature with correlation filter", Proceedings of IEEE International Conference on Digital Signal Processing, 2016: 482-486.

[11] He, X. and Liu, G. "A high-speed algorithm for particle CBMeMBer filter." IAENG International Journal of Computer Science, 2016, 43(4): 456-462.

[12] Chen, Z., Wu, C. and Zhang, Y. *et al*. "Vehicle behavior learning via sparse reconstruction with $\ell 2-\ell p$ minimization and trajectory similarity." IEEE Transactions on Intelligent Transportation Systems, 2017, 18(2): 236-247.

[13] Brendan, T. and Mohan, M. "Trajectory learning for activity understanding: unsupervised, multilevel, and long-term adaptive approach." IEEE Transactions on Pattern Analysis and Machine Intelligence, 2011, 33(11): 2287-2301.

[14] Hou, A., Guo, J. and Wang, C., *et al*. "Abnormal behavior recognition based on trajectory feature and regional optical flow", Proceedings of IEEE International Conference on Image and Graphics, 2013: 643-649.

[15] Wei, Z., Chen N, and Oh, Y.H., *et al*. "A new method for trip-line detection in surveillance video." International Journal of Signal Processing, Image Processing and Pattern Recognition, 2014, 7(2): 223-236.

[16] Harish, P., Subhashini, R. and Priya, K. "Intruder detection by extracting semantic content from surveillance videos", Proceedings of International Conference on Green Computing Communication and Electrical Engineering, 2014: 1-5.

[17] Park, J., Shin, Y. and Jeong, J., *et al*. "Detection and tracking of intruding objects based on spatial and temporal relationship of objects", Proceedings of International Conference on Information Security and Assurance, 2013, 21: 271-274.
[18] Haga, T. and Watanabe, K. "Human specific activity retrieval from a surveillance image sequence", Proceedings of International Conference on Instrumentation, Control and Information Technology, 2008: 3051-3054.
[19] Huan, R., Wang, Z and Tang, X., *et al*. "A method for wandering trajectory detection in video monitor", Proceedings of International Conference on Intelligent Robotics and Applications, 2011:116-124.
[20] Chen, Q., Wu, R., and Ni, Y., *et al*. "Research on human abnormal behavior detection and recognition in intelligent video surveillance." Journal of Computational Information Systems, 2013, 9(1): 289-296.
[21] Rai, H., Kolekar, M. and Keshav, N., *et al*, "Trajectory based unusual human movement identification for video surveillance system", Proceedings of International Conference on Systems Engineering, 2015: 789-794.
[22] Barragana, M., Alvares, L. and V, Bogorny. "Unusual behavior detection and object ranking from movement trajectories in target regions." International Journal of Geographical Information Science, 2016, 31(2): 364-386.
[23] Xu, R., Guan, Y. and Huang, Y. "Multiple human detection and tracking based on head detection for real-time video surveillance." Multimedia Tools and Applications, 2014, 74(3):729-742.
[24] Guan, Y. and Huang, Y. "Multi-pose human head detection and tracking boosted by efficient human head validation using ellipse detection." Engineering Applications of Artificial Intelligence, 2015, 37(1): 181-193.
[25] Chandola, V., Banerjee, A. and Kumar, V. "Anomaly detection – a survey." ACM Computing Surveys, 2009, 41(3): 1-58.
[26] Bertini, M., Bimbo, A. and Seidenari, L. "Multi-scale and real-time nonparametric approach for anomaly detection and localization." Computer Vision and Image Understanding, 2012, 116(3): 320-329.
[27] Wiliem, A., Madasu, V. and Boles, W., *et al*. "A suspicious behavior detection using a context space model for smart surveillance systems." Computer Vision and Image Understanding, 2012, 116(2): 194-209.
[28] Roshtkhari, M. and Levine, M. "An on-line, real-time learning method for detecting anomalies in videos using spatio-temporal compositions." Computer Vision and Image Understanding, 2013, 117(10): 1436-1452.
[29] Sharif, M. and Djeraba, C. "An entropy approach for abnormal activities detection in video streams." Pattern Recognition, 2012, 45(7): 2543-2561.
[30] Fawcett, T. "An introduction to ROC analysis." Pattern Recognition Letters, 2006, 27(8): 861-874.
[31] Kerekes, J. "Receiver operating characteristic curve confidence intervals and regions." IEEE Geoscience and Remote Sensing Letters, 2008, 5(2): 251-255.